Thin Solid Films, *95* (1982) 297–308
PREPARATION AND CHARACTERIZATION

PLASMA OXIDATION*

A. T. FROMHOLD, JR.
Physics Department, Auburn University, Auburn, AL 36849 (U.S.A.)
(Received March 22, 1982; accepted April 5, 1982)

The general assumption is made that the rate of oxidation is limited by the transport of ionic species through the already formed layer, with the transport mechanism being the thermally activated hopping of ionic defects in the presence of electric fields due to the surface potential established by the discharge and modified by the space charge of the mobile ionic defects. The results of the treatment are also applicable if the transport occurs by place exchange. Although attention in the present work is focused specifically on electrically isolated metal samples in the presence of an r.f.-excited oxygen plasma, the theoretical model is not limited in applicability to this special case.

1. INTRODUCTION

The catalytic effect of oxygen discharges on the oxidation of metals has been studied since the mid-1930s. Interest in recent years has been greatly stimulated by the manifold practical applications of thin barrier layers in areas of applied physics such as solid state electronics[1–4]. Today a great variety of techniques exists for producing oxides and similar barrier layers by the gas discharge method. Experimental variables include the magnitude and frequency of the voltage sustaining the discharge, the pressure and exact composition of the gas, and the electric potential of the metal sample being oxidized and the specific location of the metal in the discharge.

The enhanced rate promoted by the discharge may be due to a combination of several factors, such as production of a more reactive oxygen species by means of the discharge, the implantation of oxygen ions in the oxide by ion bombardment due to the discharge, and the modification of the built-in voltage across the growing oxide layer normally present during ordinary thermal oxidation. An external voltage can be impressed directly across the oxide growing in the discharge by attaching one lead of a voltage source to the parent metal and attaching the other lead of the

* Paper presented at the International Conference on Metallurgical Coatings and Process Technology, San Diego, CA, U.S.A., April 5–8, 1982.

0040-6090/82/0000-0000/$02.75

voltage source to a counterelectrode immersed in the ionized gaseous plasma produced by the discharge. If the parent metal is charged positively in this arrangement, the oxide is anodically produced in a way which is quite analogous to anodization in a liquid electrolyte[5–7].

There are many ways of producing a gaseous discharge. Either a d.c. or an a.c. discharge can be initiated. The d.c. glow discharge is experimentally simple and is useful in producing thin oxides. A higher density plasma is obtained, however, in the low pressure d.c. arc discharge. If an a.c. voltage source is used to produce the discharge, the characteristics of the discharge depend upon the frequency of the source. For example, r.f. discharges have been utilized[3,4] in studies of the formation of PbO layers on parent lead. Microwave discharges have also been utilized.

The plasma produced in the gaseous discharge is likewise characteristic of the value of the applied voltage utilized to create and maintain the discharge. Higher plasma densities often lead to higher oxide growth rates and thicker oxide films, although the sputter removal rate of the already formed oxide by ion bombardment in the discharge frequently becomes an important experimental variable. Greiner[3] was able to control dynamically the oxide thickness by balancing the sputtering rate against the growth rate. Such precise control is highly desirable in device fabrication, and it is especially critical for quantum devices involving tunneling between metals because the electron tunnel current is an extremely sensitive function of the thickness of the insulating layer separating the metals.

2. THEORETICAL MODEL

A number of important factors are changed when a metal is anodized in a gaseous plasma instead of in a liquid electrolyte. However, there is no experimental evidence which indicates any fundamental difference in the ion transport mechanism during oxide growth. Thus the simplest theoretical approach is to utilize fundamental hopping equations[7,8] for a growth rate limited by ionic transport, with the addition of a negative growth rate term to account for the effect of oxide sputtering due to bombarding ions from the plasma. As in the case of liquid anodization[7], the transport of electrons will be considered not to be rate limiting, primarily because such transport can take place readily through the external circuit for cases in which an external potential is applied to the sample. In the alternative case of a floating sample, the formulation will apply immediately only to those systems for which electron transport through the growing oxide occurs much more readily than ion transport. (As in thermal oxidation[8], both ions and electrons must be transported in order to form new charge-neutral oxide molecules.) There may be sufficient leakage currents through the plasma region surrounding the floating sample to shortcircuit the oxide for electron transport, and in this case the formulation holds even for the plasma formation of oxides which are normally better conductors of ions than of electrons.

The particle current density for the steady state hopping transport of ionic species[6,7] in strong electric fields is given by

$$J_0 = \psi \frac{DC(0)}{2a} \exp\left\{-\frac{V(L)}{E^*L(t)}\right\} \tag{1}$$

where

$$E^* \equiv k_B T/Zea \tag{2}$$

The voltage $V(L)$ across the oxide is that which exists in the presence of the oxygen plasma; it is determined by the metal oxide in question and the experimental conditions of the plasma, but it is considered to be independent of the specific value of the oxide film thickness L. The diffusion coefficient D for the mobile species with concentration C is determined by the microscopic parameters of the oxide[7,8], such as the hopping distance $2a$. The concentration $C(0)$ of the mobile ionic species is the value at the interface with the higher defect density; for oxygen interstitials or cation vacancies this would be the oxide–plasma interface, whereas for cation interstitials or anion vacancies this would be the metal–oxide interface. The parameter ψ, which determines the space charge retardation of the growth rate, is determined from

$$\ln \psi \equiv 1 - \frac{x^*}{L}\left(1+\frac{L}{x^*}\right)\ln\left(1+\frac{L}{x^*}\right) \tag{3}$$

where

$$x^* \equiv \frac{\varepsilon k_B T}{4\pi (Ze)^2 C(0) a} \tag{4}$$

The charge of the mobile defect ion is denoted by Ze, the static dielectric constant of the growing oxide is denoted by ε, and $k_B T$ is the thermal energy at temperature T.

The net growth rate $\mathrm{d}\{L(t)\}/\mathrm{d}t$ of the oxide with time t is determined by the dynamic balance between the positive contribution J_0 due to oxide growth and the negative (reverse) contribution J_{rev} due to oxide sputtering:

$$\frac{\mathrm{d}\{L(t)\}}{\mathrm{d}t} = R(J_0 - J_{rev}) \equiv RJ_{tot} \tag{5}$$

where R is the molecular volume of oxide associated with each ion which is transported through the oxide. The integral of the net (total) current density J_{tot} gives the formal expression for oxide thickness $L(t)$ as a function of time t, *i.e.*

$$t = \int_{L(0)}^{L(t)} (RJ_{tot})^{-1}\,\mathrm{d}L \tag{6}$$

Numerical evaluations of this expression for the plasma oxidation kinetics utilizing typical values for the microscopic parameter values have been carried out[9]. In this way, parametric curves have been developed to evaluate the general predictions of the model. These curves illustrate the dependence of oxide growth kinetics on the various microscopic parameters (the activation energy for charged defect motion, the concentration of the mobile ionic defect species and the dielectric constant of the oxide) and on the other variables of the system (the electrostatic potential difference across the oxide layer, the sputtering rate and the temperature of the sample). Typical results are shown in Section 3.2, and an application of the results to experimental data[4] on the r.f. plasma oxidation of lead is shown in Section 3.3.

An interesting and important feature of plasma oxidation is the limiting oxide thickness achieved under dynamic growth and sputtering conditions. Equation (5) predicts that the growth rate $\mathrm{d}\{L(t)\}/\mathrm{d}t$ can be either positive or negative, and that it

will be zero when the oxide thickness $L(t)$ reaches the specific thickness L_∞ such that

$$J_0|_{L(t)=L_\infty} = J_{rev} \tag{7}$$

This thickness, which is referred to as the "steady state limiting thickness", is theoretically achieved only when the time t approaches infinity but, because the laboratory time constant is typically in the range of 100–1000 s for the asymptotic approach of $L(t)$ to L_∞, effectively the limiting thickness is achieved after 20 min or so of plasma anodization.

Equation (7) is found to be useful in a number of ways. For example, it can be evaluated at any given thickness, using eqn. (1), to ascertain the level of sputtering current which must be chosen to yield that value for the limiting thickness. Alternatively, if we wish to know the voltage across the oxide layer which will yield a given value of the limiting thickness for some fixed sputtering current, eqn. (7) can be evaluated by means of eqn. (1) and rearranged to yield

$$V(L_\infty) = \frac{k_B T L_\infty}{Zea}\left[\ln\left\{\frac{DC(0)}{2aJ_{rev}}\right\} + \ln\psi|_{L(t)=L_\infty}\right] \tag{8}$$

Often it is desirable to be able to predict the limiting thickness L_∞, given specific values for all other variables in the theory. Although eqn. (7) cannot be solved explicitly for L_∞, a useful implicit expression can be readily obtained:

$$L_\infty = \frac{ZeaV(L)}{k_B T}\left[\ln\left\{\frac{DC(0)}{2aJ_{rev}}\right\} + \ln\psi|_{L(t)=L_\infty}\right]^{-1} \tag{9}$$

The results of an iterative evaluation of this implicit expression for a number of sets of microscopic parameter values are shown in Section 3.4.

3. NUMERICAL EVALUATION OF PLASMA OXIDATION KINETICS

3.1. *Microscopic parameter values*

Since there are a number of microscopic parameters in the theory, it is necessary to adopt a systematic method for studying the effects of varying the values of one or another of these parameters. Extensive data on the r.f. plasma oxidation of lead is readily available[4], so parameter values typical of PbO (Tables I and II) were chosen for the initial computations. The effects of varying the most important of these parameters were then studied by generating parametric families of growth curves by numerical evaluation of eqn. (6).

3.2. *Parametric families of growth curves*

Figure 1 illustrates a family of three curves with temperature constituting the parametric variable. These curves were generated by incrementing the temperature from curve to curve, the remaining microscopic parameter values being held fixed at the values listed in Tables I and II. The "runaway" behavior of the higher temperature curve is particularly interesting, since it offers the possibility that oxide formation can be self-catalytic if it is not carried out under isothermal conditions. The predominant temperature dependence (and activation energy dependence) of the families of curves can be attributed to the ratio $W/k_B T$ appearing as an argument of the exponential factor in eqn. (1). This is not quite the entire picture, however,

TABLE I
FIXED MICROSCOPIC PARAMETER VALUES UTILIZED IN MODELING PbO GROWTH KINETICS

Symbol	*Units*	*Terminology*	*Value*
T	K	Temperature	297
Z	—	Valence of mobile species	−2
$2a$	Å	Lattice parameter (hopping distance)	2.946
R	Å^3	Volume of PbO formed per ionic defect transported through the oxide layer	38.45
ν	s^{-1}	Hopping attempt frequency	10^{13}
ε	—	Low frequency dielectric constant of PbO relative to the permittivity ε_0 of free space	30

TABLE II
TYPICAL PARAMETER VALUES FOR ADJUSTABLE CONSTANTS IN FITTING THEORY

Symbol	*Units*	*Terminology*	*Value*
W	eV	Activation energy for diffusion of mobile defect species	0.75
$C(0)$	cm^{-3}	Bulk defect concentration at the oxide interface	10^{21}
$V(L)$	V	Electrostatic potential drop across the oxide layer	1.6
J_{rev}	cm^{-2} s^{-1}	Oxide sputtering rate in terms of the mobile ionic species	1.8×10^{13}

because of the additional temperature dependence arising from the electric field modification of the current. As can be noted from eqn. (1), the ratio $ZeEa/k_BT$ also appears as an argument in the exponential factors involved in the hopping current expression.

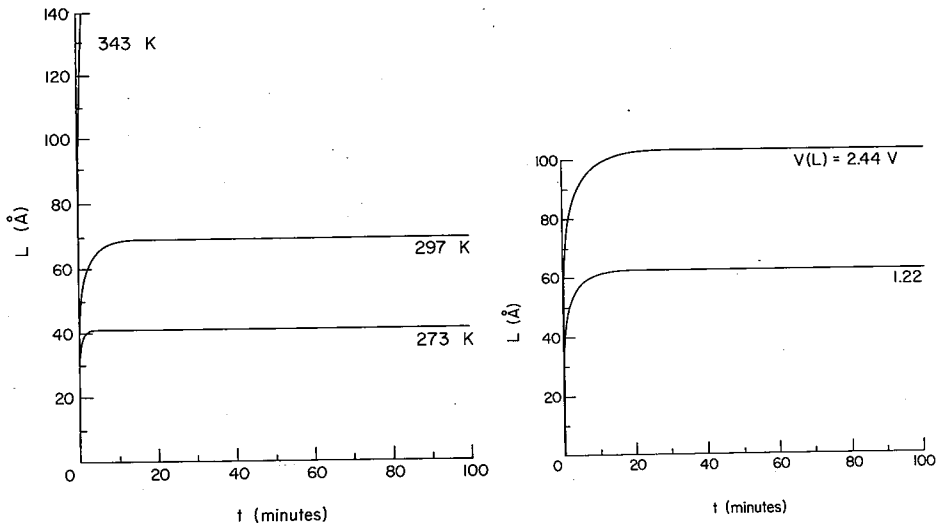

Fig. 1. Family of theoretical kinetics curves with temperature constituting the parametric variable. (See Tables I and II for those parameter values not listed in the figure.)

Fig. 2. Family of theoretical kinetics curves with electrostatic potential difference constituting the parametric variable. (See Tables I and II for those parameter values not listed in the figure.)

Figure 2 shows a pair of growth curves obtained by doubling the voltage across the oxide layer and keeping all other parameter values fixed at the values listed. It can be readily noted that these theoretical curves consist of a fast rise portion followed by a portion corresponding to the limiting thickness. The sputtering rate affects principally the regions of the growth curves corresponding to the limiting thickness. Although the "forward" current produced by the voltage greatly exceeds the "reverse" current due to the sputtering in the early growth stages, the currents become comparable and finally equal in magnitude as the dynamic limiting thickness is approached. The kinetic curves depend sensitively upon the values of the microscopic parameters utilized in the evaluation, since these values determine the rate of movement of the charged ionic defects through the already grown layer thickness. The variation in the limiting thickness with the value of each of several microscopic parameters is studied in Section 3.4.

3.3. R.f. oxidation of lead

The ready availability of experimental data on the r.f. plasma oxidation of lead[4] motivated the initial choice of parameter values (Tables I and II). This section is concerned primarily with theoretical fits of the theory to these published data. In addition to r.f. plasma oxidation studies, several thermal oxidation studies have been carried out[10–12]. Also, experimental data for the transport of lead and oxygen defect species in PbO have been published[13–15]. Structural studies of oxides on lead have also been made[16,17].

The literature data of primary interest to us in this work were those of Greiner[4] for the r.f. oxidation of lead films, 4000 Å in thickness, deposited onto oxidized silicon wafers. It has been shown that such films grow with a preferred orientation such that the majority of the lead grains in the film are oriented with their (111) plane parallel to the plane of the surface[18]. Both thermal and r.f.-grown oxides on such films have been shown[16,19] to be predominantly crystalline orthorhombic PbO oriented with the (001) plane of PbO parallel to the surface. Furthermore, the PbO crystallites were shown[17] to have an orientational preference with respect to the crystallographic directions in the plane of the film, even though the alignment is not sufficiently close to regard the PbO as being epitaxial on the lead. The parameter R (representing the volume of a PbO molecule), the lattice constant $2a$ and the dielectric constant ε were chosen assuming orthorhombic (001)-oriented PbO. With these considerations in mind, the parameter values listed in Table I were used for the Pb/PbO system. Listed in Table II are the parameter values which were chosen somewhat more arbitrarily (though realistically), since precise experimental values were not available. Some of the considerations behind the initial choice for these values are discussed in ref. 9.

If the assumption of an ionic transport rate-limiting mechanism is correct, some mechanism must be postulated by which electrons (or other negatively charged species) move from the oxidizing metal to the surface of the oxide adjacent to the plasma to compensate the opposite charge transported across the oxide by the diffusing ions. If the metal were electrically connected to another part of the system, an external path across the oxide would be established via the plasma. However, for a truly floating sample, this is not the case: the compensating charge must be transported through the oxide. It was proposed[9,20] that in the case of lead this takes

place by the creation of electron holes at the oxide surface by ion neutralization, and that these holes readily migrate under a concentration gradient through the oxide to the metal, thus effectively transporting an electron from the metal to the oxide surface. This hole creation by ion neutralization is possible since the incoming O^+ ions, for example, have an unoccupied level about 13 eV below the vacuum level, or 8 eV below the Fermi level (assuming a 5 eV work function). This is well below the valence band edge for most oxides, and thus it is energetically possible for an electron from the valence band to fill the unoccupied level in the ion. This contrasts with thermal oxidation[8, 12], where only the oxygen affinity level is available to the electrons. If the affinity level is not sufficiently low to accept electrons from the valence band, then electrons from the Fermi level must traverse the oxide with a much lower probability via tunneling[21] or else be thermally excited to the conduction band of the oxide with subsequent transport by a conduction band mechanism[22]. This may be the reason why thermal oxidation occurs so much more slowly than plasma oxidation.

The voltage across the oxide layer is believed to arise from a surface charge of excess negative oxygen ions. That is, oxygen is adsorbed as neutral or positively charged oxygen atoms from the discharge, and these subsequently become negatively ionized on (or just beneath) the surface of the oxide. A dynamic balance between the concentration of these oxygen ions and the injected electron holes could then determine the voltage across the oxide. The fact that voltages as high as 1–2 eV are observed[20] across the oxide suggests that the hole concentration is very high at the surface. This is consistent with the high levels of excess oxygen observed at the surface by Auger spectroscopy and indicated by the continued growth of the oxide after the plasma oxidation has been terminated[20]. If this high concentration of oxygen ions were not largely compensated by the electron holes, a much higher voltage than is observed or deduced from comparison of the experimental data with the theory would exist across the oxide. Thus the diffusion of ions through the oxide is considered to be field assisted in r.f. oxidation, but the fixed voltage across the oxide is controlled by the combined properties of the plasma and the oxide surface instead of by an external voltage applied to the sample.

Figure 3 illustrates a comparison between present theory and data on the r.f. oxidation of lead (ref. 4, Fig. 5) taken at 24 °C at a peak-to-peak voltage of 340 V. The set of four experimental curves were taken at different oxygen pressures. The shape of the kinetics curves predicted from the numerical evaluation of eqn. (1) and its integration in accordance with eqn. (5) is identical with that obtained experimentally. The quality of the theoretical fits is quite high for all four curves. The parameter values which were utilized are listed in Table III. The increase in limiting thickness with increased values of the oxygen pressure is not too surprising. The increased voltages across the oxide deduced by the fitting procedure (Table III) indicate that the major effect of increases in oxygen pressure on the kinetics may be to increase the built-in voltage across the oxide, which in turn provides a larger electric field to increase the rate of ion transport through the oxide layer. Other comparisons of the theory with the data of Greiner are given in ref. 9. Some consideration is also given therein to the range of parameter values which can be utilized to obtain a match between theory and experiment.

Although we can hardly attempt to correlate experimental data and theory

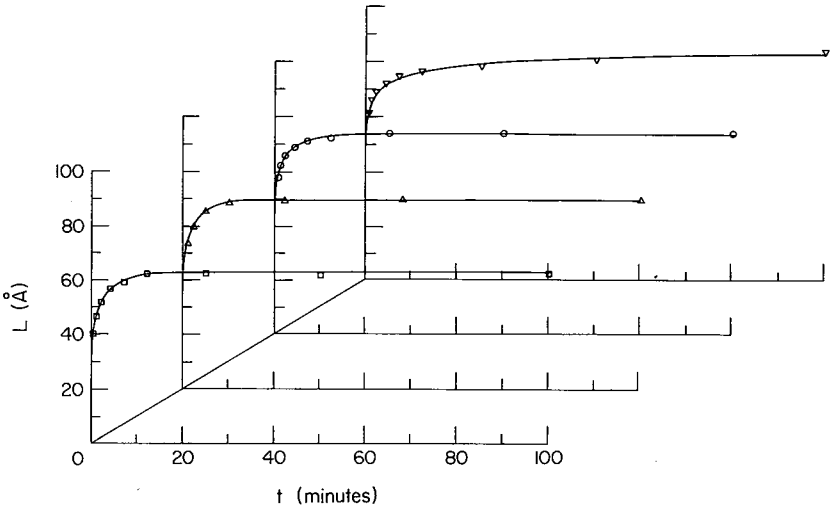

Fig. 3. Linear plots of computed (——) r.f. oxide film thickness *vs.* time of oxidation with the microscopic parameter values chosen to yield optimum least-squares fits to the data points of Greiner[4] on lead at 297 K and a peak-to-peak r.f. voltage of 340 V with oxygen pressures of 5 mTorr (□), 10 mTorr (△), 20 mTorr (○) and 40 mTorr (▽). (The microscopic parameter values are listed in Tables I and III.)

TABLE III

PARAMETER VALUES[a] UTILIZED FOR THEORETICAL FITS TO THE GROWTH KINETICS OF PbO[b]

Experimental O_2 pressure (mTorr)	*Microscopic parameter values*		
	W(eV)	$V(L)$ (V)	J_{rev} ($\times 10^{13}$ cm^{-2} s^{-1})
5	0.750	1.22	1.48
10	0.753	1.58	1.75
20	0.868	4.00	0.71
40	1.030	6.93	0.10

[a] For all curves represented in this table, the value of $C(0)$ was fixed at 10^{21} cm^{-3}.
[b] Measured by Greiner[4] at an r.f. peak-to-peak voltage of 340 V.

without raising the important question of the uniqueness of the fit, the salient point to be made is that the basic shape of the theoretical curves is not altered appreciably by changing the parameter values, even though the time scale and (to a lesser extent) the thickness scale may be dramatically altered by changing certain parameter values. Because only the scales and not the shape of the theoretical growth curves are amenable to alteration by the choice of parameter values, the agreement found between theory and experiment is significant.

3.4. Dynamic steady state limiting thickness

Because device technology is extremely demanding with regard to the precise thickness of insulating layers, reliable predictions of oxide thickness variations produced by changes in the microscopic parameter values, the temperature, the voltage developed across the oxide and the sputtering current are extremely

important. The dependence of the limiting oxide thickness on these variables is illustrated in this section by iterative evaluations of eqn. (9). The procedure adopted is to plot the limiting thickness continuously *versus* one microscopic parameter value, with a second microscopic parameter value incremented to generate a parametric set of curves.

One parametric set of curves is shown in Fig. 4 where the limiting thickness L_∞ is plotted *versus* the ambient temperature T for five different voltages across the layer. A quasi-exponential increase in the limiting thickness with increasing temperature is apparent from this figure. In addition, the greater limiting thicknesses which accompany increasing values of the voltage at any given temperature should be noted. In a similar way, there is a sensitive dependence of the limiting thickness on the value of the activation energy, with decreased activation energies yielding larger limiting thicknesses at a given temperature[9].

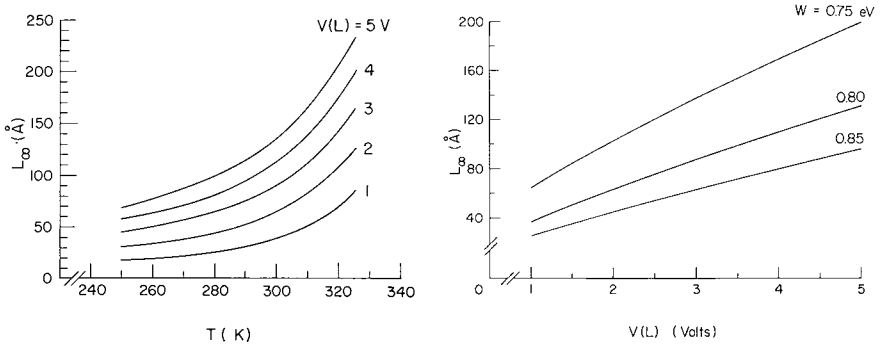

Fig. 4. Computed values of limiting thickness *vs.* temperature with electrostatic potential difference as the parametric variable ($W = 0.80$ eV; $J_{rev} = 10^{13}$ cm^{-2} s^{-1}; $2a = 2.95$ Å; $C(0) = 10^{21}$ cm^{-3}; values of ε, Z, R and ν as listed in Table I).

Fig. 5. Computed values of limiting thickness *vs.* electrostatic potential difference with activation energy as the parametric variable ($J_{rev} = 10^{13}$ cm^{-2} s^{-1}; $2a = 2.95$ Å; $C(0) = 10^{21}$ cm^{-3}; T, Z, R and ν as in Table I).

Figure 5 illustrates L_∞ *versus* voltage $V(L)$ for three different activation energies. Figure 6, illustrating L_∞ *versus* $V(L)$ for four different temperatures, gives further insight into the interplay between voltage and temperature increases. Figure 7 illustrates the rise in the L_∞ *versus* $V(L)$ curve which is predicted for increased oxygen defect densities. Another set of computations (not illustrated herein) was carried out to ascertain L_∞ for different values of the hopping distance $2a$. It was found that increases in $2a$ led to increased values for L_∞. This can be understood as follows: increased values of $2a$ lead to greater field modifications in the potential energy barrier heights, which then result in greater values of the "forward" current.

Figure 8 shows L_∞ *versus* J_{rev} for three different activation energies in order to give insight into the interplay between activation energy modifications in the "forward" current and the sputtering rate expressed as a "reverse" current density. Another set of computations (not illustrated herein) was carried out to study the effect of the ionic point defect charge Ze on L_∞. It was found that an increase in the magnitude of Z leads to a greater "forward" current for a given thickness and

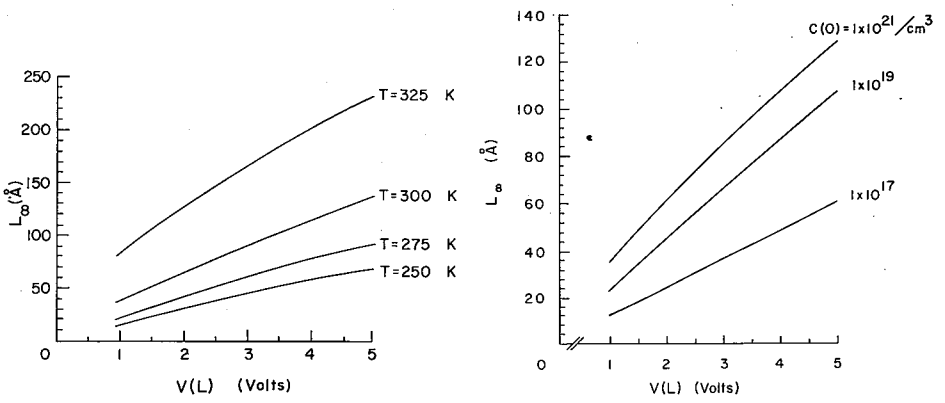

Fig. 6. Computed values of limiting thickness *vs.* electrostatic potential difference with temperature as the parametric variable ($W = 0.80$ eV; $J_{rev} = 10^{13}$ cm^{-2} s^{-1}; $2a = 2.95$ Å; $C(0) = 10^{21}$ cm^{-3}; Z, R and v as in Table I).

Fig. 7. Computed values of limiting thickness *vs.* electrostatic potential difference with mobile oxygen ion concentration as the parametric variable ($W = 0.80$ eV; $J_{rev} = 10^{13}$ cm^{-2} s^{-1}; $2a = 2.95$ Å; T, Z, R and v as in Table I).

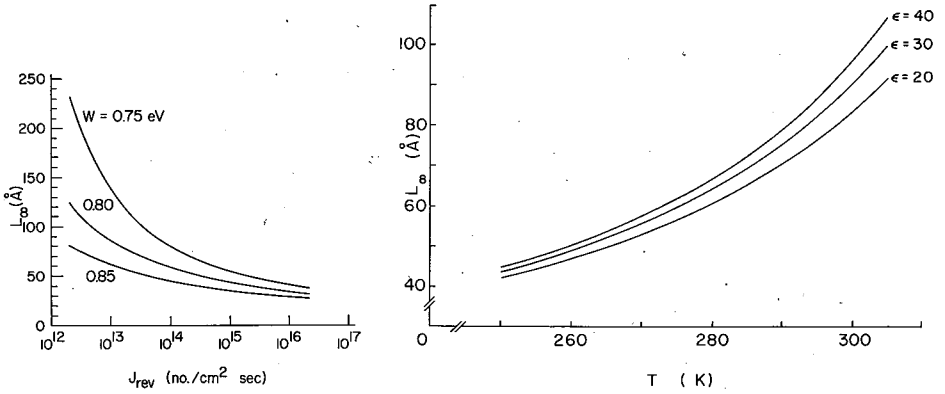

Fig. 8. Computed values of limiting thickness *vs.* sputtering current density with activation energy as the parametric variable ($V(L) = 3$ V; $2a = 2.95$ Å; $C(0) = 10^{21}$ cm^{-3}; T, Z, R and v as in Table I).

Fig. 9. Computed values of limiting thickness *vs.* temperature with static dielectric constant as the parametric variable ($W = 0.80$ eV; $V(L) = 3$ V; $J_{rev} = 10^{13}$ cm^{-2} s^{-1}; $2a = 2.95$ Å; $C(0) = 10^{21}$ cm^{-3}; Z, R and v as in Table I).

voltage, which in turn leads to increases in L_∞ at a given sputtering current density J_{rev}.

Figure 9 shows L_∞ *versus* T for three different values of the static dielectric constant. It can be noted that larger values of the dielectric constant lead to larger values for the limiting thickness. This is to be understood in terms of the space charge retardation of the growth rate of the oxide: a given level of space charge yields a lower value for the electric field the larger the static dielectric constant is, in accordance with Poisson's equation, and this in turn causes a given level of space charge to be less effective in retarding the growth rate of the oxide layer[7]. Of course, the larger the growth rate at a given thickness, the larger is the thickness required for a dynamic balance between the growth rate and a given sputtering rate.

Figure 10 illustrates the functional dependence of L_∞ on the diffusing oxygen defect concentration $C(0)$. These computations of L_∞ *versus* $C(0)$ for four different temperatures illustrate the interdependence between the effects of temperature and oxygen point defect concentration. The curves show an initial increase in L_∞ with $C(0)$ followed by an asymptotic approach to L_∞ values which are independent of $C(0)$. This behavior is to be understood as follows: in the small space charge limit (low $C(0)$ limit), space charge retardation effects are negligible and an increase in $C(0)$ results in a corresponding increase in the ionic conductivity $Ze\mu C$ and thus an increase in the "forward" ionic current[8]. As $C(0)$ increases to very large values, however, the space charge of the mobile oxygen ions produces a greater and greater retardation of the ionic current[7] until finally the two contrary effects cancel one another, thereby yielding the flat (asymptotic) portions of the curves.

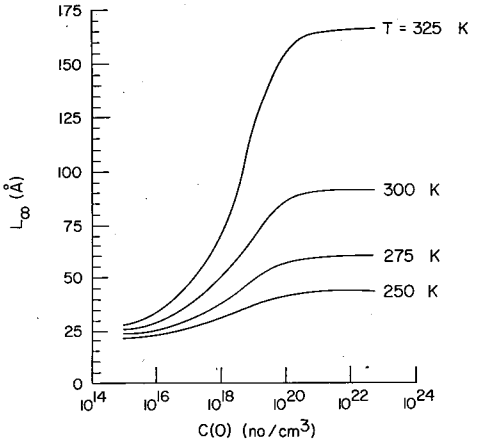

Fig. 10. Computed values of limiting thickness *vs.* mobile ion defect concentration with temperature as the parametric variable ($W = 0.80$ eV; $V(L) = 3$ V; $J_{rev} = 10^{13}$ cm^{-2} s^{-1}; $2a = 2.95$ Å; Z, R and ν as in Table I).

4. CONCLUSIONS

A theoretical model has been developed to analyze specific data in the literature on plasma oxidation[9]. The general assumption was made that the rate of oxidation is limited by the transport of ionic species through the already formed layer, with the transport mechanism being the thermally activated hopping of ionic defects (or else place exchange[23]) in the presence of electric fields due to the surface potential established by the discharge and modified by the space charge of the mobile ionic defects.

Specifically in the case of PbO films produced on lead[9], the origin of the voltage was assumed to be a balance between the transport of negatively charged oxygen ions and the transport of electron holes created by ion neutralization of positive ions from the plasma. The model was developed analytically and evaluated numerically by employing the continuum limit of the hopping transport equations valid for the very high field limit[9]. A three-parameter fit (namely the voltage across the oxide film, the ionic diffusivity and the rate of oxide removal by sputtering) gave excellent agreement with the published data of Greiner[4]. Moreover, the deduced parameter

values were in good agreement with those available from independent experimental data[9]. The electric field developed across the PbO arises from negatively charged oxygen ions near the surface of the oxide, with the space charge field due to the mobile ions producing a significant retardation in the growth rate of the oxide[9].

Parametric curves were developed to evaluate the general predictions of the model. These curves illustrated the dependence of oxide growth kinetics on the various microscopic parameters (the activation energy for charged defect motion, the concentration of the mobile ionic defect species and the dielectric constant of the oxide) and on the other variables of the system (the electrostatic potential difference across the oxide layer, the sputtering rate and the temperature of the sample). The model was found to predict a very rapid initial growth rate which decreases markedly with increasing thickness until some steady state limiting thickness is reached. This limiting thickness was predicted to be a sensitive function of several of the microscopic parameters and experimental variables of the system. A separate set of parametric curves was generated to illustrate the dependence of the limiting thickness on the microscopic parameters of the system.

ACKNOWLEDGMENT

This research was performed in collaboration with Dr. John M. Baker, IBM Thomas J. Watson Research Center, Yorktown Heights, NY 10598, U.S.A.

REFERENCES

1 C. J. Dell'Oca, D. L. Pulfrey and L. Young, *Phys. Thin Films, 6* (1971) 36–51.
2 J. F. O'Hanlon, in A. K. Vijh (ed.), *Oxides and Oxide Films*, Vol. 5, Dekker, New York, 1977, pp. 105–166.
3 J. H. Greiner, *J. Appl. Phys., 42* (1971) 5151.
4 J. H. Greiner, *J. Appl. Phys., 45* (1974) 32.
5 A. T. Fromhold, Jr., and J. Kruger, *J. Electrochem. Soc., 120* (1973) 722.
6 A. T. Fromhold, Jr., *J. Electrochem. Soc., 124* (1977) 538.
7 A. T. Fromhold, Jr., Space charge effects on anodic film formation, in J. W. Diggle and A. K. Vijh (eds.), *Oxides and Oxide Films*, Vol. 3, Dekker, New York, 1976, pp. 1–271.
8 A. T. Fromhold, Jr., *Theory of Metal Oxidation*, Vol. I, *Fundamentals*, North-Holland, Amsterdam, 1976, Chap. 8.
9 A. T. Fromhold, Jr., and J. M. Baker, *J. Appl. Phys., 51* (1980) 6377.
10 J. M. Eldridge and D. W. Dong, *Surf. Sci., 40* (1973) 512.
11 M. G. Hapase, M. K. Gharpurey and A. B. Biswas, *Surf. Sci., 12* (1968) 85.
12 J. M. Baker and A. T. Fromhold, Jr., *Bull. Am. Phys. Soc., 21* (1976) 321.
13 R. Lindner, *Ark. Kemi, 4* (1952) 385.
14 B. A. Thompson and R. L. Strong, *J. Phys. Chem., 67* (1963) 594.
15 L. Heyne, N. M. Beekmans and A. de Beer, *J. Electrochem. Soc., 119* (1972) 77.
16 T. B. Light, J. M. Eldridge, J. W. Matthews and J. H. Greiner, *J. Appl. Phys., 46* (1975) 1489.
17 J. W. Matthews, C. J. Kircher and R. E. Drake, *Thin Solid Films, 42* (1977) 69.
18 S. K. Lahiri, *J. Appl. Phys., 41* (1970) 3172.
19 J. M. Baker, R. W. Johnson and R. A. Pollak, *J. Vac. Sci. Technol., 16* (1979) 1534.
20 J. M. Baker, personal communication, 1978.
21 A. T. Fromhold, Jr., *Theory of Metal Oxidation*, Vol. I, *Fundamentals*, North-Holland, Amsterdam, 1976, Chap. 10.
22 A. T. Fromhold, Jr., *Theory of Metal Oxidation*, Vol. I, *Fundamentals*, North-Holland, Amsterdam, 1976, Chap. 11.
23 A. T. Fromhold, Jr., *J. Electrochem. Soc., 127* (1980) 411.